East European Journal of Physics. 2. 482-490 (2026)
DOI:10.26565/2312-4334-2026-2-54 ISSN 2312-4334

OPTIMIZATION OF MULTILAYER GRAPHENE-BASED ABSORBERS UNDER H-POLARIZATION VIA DIFFERENTIAL EVOLUTION IN A HYBRID COMPUTING ENVIRONMENT

Mstyslav E. Kaliberda[1,2]*, Sergey A. Pogarsky[1,2], Vladyslav M. Nasonov[1], Viktoriia A. Lunova[1]
[1]*V. N. Karazin Kharkiv National University, 4, Svobody Sq., Kharkiv, Ukraine, 61022*
[2]*Institute of Radio Astronomy of NAS of Ukraine, 4, Mystetstv St. Kharkiv, Ukraine, 61002*
**Corresponding Author e-mail: KaliberdaME@gmail.com*
Received February 20, 2026; revised March 29, 2026; accepted May 24, 2026

A computationally efficient framework for optimizing multilayer radar-absorbing structures based on periodic planar gratings of resistive strips embedded in a dielectric slab is presented for the *H*-polarization case. The electromagnetic response is modeled using a rigorous singular integral equation (SIE) formulation combined with an operator-based cascading technique, providing high numerical accuracy and stability with low computational cost. This ultra-fast forward solver is integrated into a parallel differential evolution (DE) optimization framework implemented in a client–server architecture, enabling efficient solution of high-dimensional inverse design problems. The optimization targets broadband absorption under normal incidence while preserving optical transparency, with graphene used as a representative resistive material. Numerical results demonstrate effective suppression of resonance-induced spectral holes and stable, wideband absorption in multilayer structures with 10 layers, showing robustness under fabrication-inspired constraints and oblique incidence.
Keywords: *Graphene; Wideband absorber; Differential evolution; Singular integral equations; Multilayer periodic structure; Global optimization*
PACS: 42.25.Bs, 02.60.Pn, 02.30.Rz, 07.05.Tp

INTRODUCTION

The ability to lower the radar visibility of various platforms is essential for their protection in modern high-threat environments. The mitigation of radar cross-section (RCS) directly determines the operational survivability of these assets [1]. This reduction in radar signatures can be achieved by optimizing sophisticated structural configurations, such as multi-layered systems, capable of broadband absorption. Beyond stealth applications, absorbing materials are essential for ensuring the electromagnetic compatibility of electronic equipment, protecting biological entities from electromagnetic radiation, and eliminating reflections in anechoic chambers [2]. However, many of the proposed absorber designs rely on complex geometries and fabrication techniques that are difficult to implement in practice, especially under constrained industrial or real-world field -deployment conditions. This motivates the development of structurally simple, scalable, and computationally efficient absorber designs. In recent years, graphene-based structures have attracted particular interest due to their unique surface conductivity, mechanical flexibility, and optical transparency, which open new possibilities for multifunctional devices. The present study focuses on the efficient optimization of the scattering and absorption characteristics of an infinite periodic multilayer grating of resistive strips, enabled by our home-made ultra-fast rigorous electrodynamic solver. The emphasis is not on proposing new exotic absorber geometry, but on demonstrating a computationally efficient optimization framework suitable for structurally simple and scalable designs.

Designing an efficient wideband device, be it an absorber, focuser, or radiator, is a non-trivial task that requires solving a complex multi-parameter optimization problem. The primary objective of this research is to achieve maximum absorption over a broad frequency band while maintaining the structure's optical transparency for H-polarization. From a computational perspective, this problem is a high-dimensional inverse design task, in which each additional layer introduces multiple strongly coupled geometric and material parameters. This requirement is dictated by the potential use of such absorbers as transparent shielding coatings for aircraft cockpit canopies or protective glass for optical sensors, where graphene interacts effectively with microwave radiation without obstructing visibility in the visible range. Although graphene is used as a representative resistive material, the proposed optimization framework and solver are applicable to a wide class of resistive or impedance-type surfaces. To ensure modeling accuracy, the dielectric medium hosting the multilayer grating is assumed to be lossless. The solution to this electrodynamic problem is implemented via a hybrid computational framework built on a client-server architecture. This approach separates the global search logic from the intensive numerical kernel, enabling efficient parallelization of the rigorous singular integral equation (SIE) method and the operator method [3], [4] across multiple computing nodes. This methodology significantly reduces the dimensionality of the resulting system of linear algebraic equations by decomposing the complex problem into stages, while the stochastic nature of the optimization algorithm enables the simultaneous analysis of high-dimensional search spaces. A key advantage of this approach is the explicit incorporation of the edge

Cite as: M.E. Kaliberda, S.A. Pogarsky, V.M. Nasonov, V.A. Lunova, East Eur. J. Phys. 2, 482 (2026), https://doi.org/10.26565/2312-4334-2026-2-54

condition, which accounts for the singular behavior of the electromagnetic field at the boundaries of the graphene strips. Unlike approximate approaches based on equivalent circuit models [5] or commercial codes based on finite-element method, this rigorous formulation ensures high numerical convergence and accuracy, which is essential for the precise modeling of multilayer graphene-based structures.

In such electrodynamic problems, classical optimization methods, such as gradient descent, often fail. Typically non-convex objective functions lead to stagnation in local minima. To overcome these topological challenges, the differential evolution (DE) algorithm is used [6].

While DE is a robust global search tool [6], its performance is often enhanced through specialized strategies. Recent advancements include perturbation estimation for complex Pareto fronts [7], self-adaptive mutation strategies to handle noisy functions [8], and multi-strategy approaches to prevent premature convergence [9]. The versatility of DE extends beyond electromagnetics, proving effective in training high-gain controllers [10] and optimizing magnetic sensor placement [11].

In applied electrodynamics, the current trend shifts toward hybridizing DE with surrogate modeling and machine learning to accelerate the design of ultra-wideband antennas [12], [13], slow-wave structures [14], and textile metasurfaces [15]. Neural networks are frequently employed to assist DE in learning variable patterns [16] or to replace computationally expensive simulations [17]. Despite the popularity of approximate transmission line models for absorbers [5], our approach prioritizes a rigorous SIE formulation. By leveraging an in-house developed, ultra-fast solver combined with a parallelized client-server framework, we bypass the need for surrogate models.

PROBLEM FORMULATION AND OPTIMIZATION GOALS

Consider a multilayer periodic structure consisting of N dielectric layers separated by infinite graphene strip gratings. The entire stack is situated in a Cartesian coordinate system (x, y, z), where the z-axis is directed along the infinite graphene strips, and the z-axis is normal to the layers (see Fig. 1). All gratings share a common period l along the y-axis, which allows the structure to be treated as a single periodic system. However, the geometric parameters of each layer are independent: the n-th layer, $n = 1, 2, ..., N$ is characterized by the strip width $2d_n$, and the chemical potential of the graphene μ_{cn}. The distance between the n-th and $(n+1)$-th gratings is Δ_n, the distance from the vacuum-dielectric interface to the first grating is h. The structure is illuminated by an H-polarized plane electromagnetic wave incident from the upper half-space ($z > 0$) at an angle θ relative to the normal. The structure is infinite along the x-axis. The magnetic field vector of the incident wave is directed along the strips (the x-axis):

$$H_x^i(y,z) = \exp(-ik_0(y\sin\theta + z\cos\theta)), \tag{1}$$

where $k_0 = 2\pi/\lambda$ is the wavenumber in free space, and the time dependence is assumed to be $\exp(-i\omega t)$.

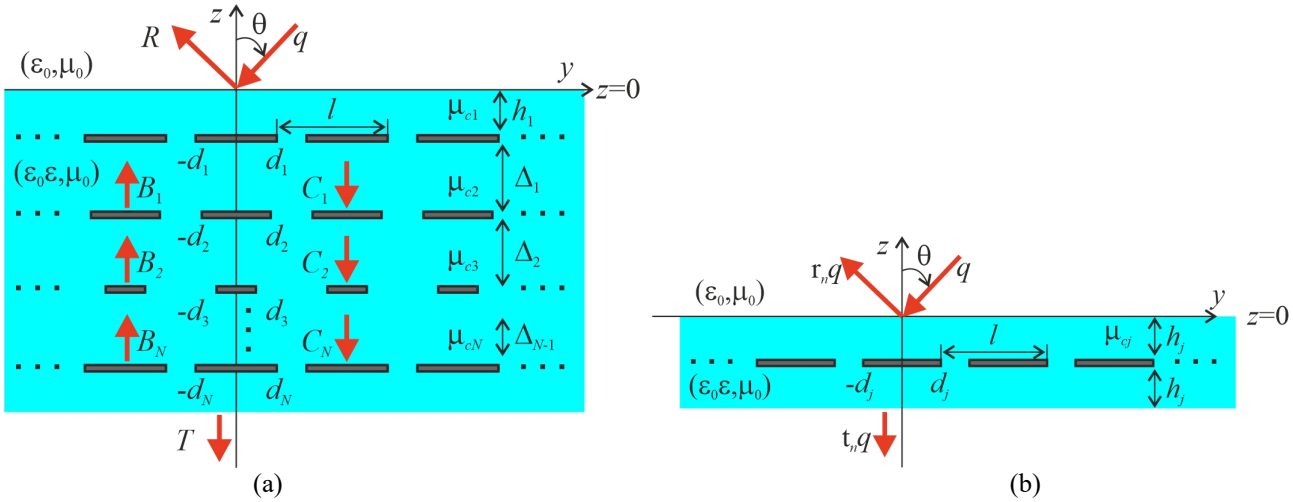

Figure 1. Structure geometry. (a) Multilayer structure, (b) single layer.

Graphene is modeled as an infinitesimally thin conductive sheet with a surface conductivity $\sigma = (f, \mu_c, \tau, T)$, calculated using the Kubo formula, which includes both intraband and interband transitions [18], [19]. Here, f is the frequency, τ is relaxation time, and T is the temperature. In our model, graphene strips are treated as resistive boundaries imposing a discontinuity in the tangential magnetic field proportional to the surface current density and continuity of the tangential electric field component:

$$E_y^+ = E_y^-, \text{ in the plane of strips,} \tag{2}$$

$$H_x^+ - H_x^- = \sigma E_y^+, \text{ on graphene strips.} \tag{3}$$

Here, the superscripts "+" and "–" denote the field values on the upper and lower sides of the graphene strip, respectively.

The primary objective of the optimization is to design a structure that acts as a wideband absorber in the microwave range while maintaining optical transparency. Since optical transparency is inherent to the material choice (graphene and transparent dielectrics), the optimization routine focuses on maximizing the absorbance $A(f)$ in the target frequency band $[f_{\min}, f_{\max}]$ under normal incidence, $\theta = 0^{\circ}$. The absorbance is defined as $A = 1–R–T$, where R and T are the power reflection and transmission coefficients, respectively. Thus, the problem is reduced to finding the optimal vector of parameters $\mathbf{P} = (h, \Delta_1,..., \Delta_{N-1}, d_1,..., d_N, \mu_{c1},..., \mu_{cN})$ that minimizes the following cost function:

$$F(\mathbf{P}) = \int_{f_{\min}}^{f_{\max}} S(A(f, \mathbf{P}))df \,, \tag{4}$$

where $S(x)$ is local scoring or penalty function.

The search space is constrained by physical realizability and fabrication limits, such as minimum strip width and feasible doping levels.

NUMERICAL MODELING STRATEGY

The electromagnetic simulation of the proposed structure is performed using a hybrid scheme that combines a rigorous SIE method for individual layers and an operator-based cascading technique for multilayer systems.

Scattering Matrix of a Single Layer

First, let us consider an auxiliary problem of diffraction by the n-th individual periodic grating embedded in a dielectric slab of width h_n, characterized by a strip width of $2d_n$, a period l, and a graphene chemical potential μ_{cn}. Following the rigorous derivation presented in our previous work [3], the problem is reduced to finding the unknown function $F(\xi)$, which is related to the derivative of the surface current density on graphene strips. The enforcement of boundary conditions leads to SIE of the first kind with a Cauchy-type kernel:

$$\frac{1}{\pi} PV \int_{-\delta}^{\delta} \frac{F(\xi)}{\xi - \psi} d\xi + \frac{1}{\pi} \int_{-\delta}^{\delta} K(\psi, \xi) F(\xi) d\xi = -\frac{l}{2\pi} \frac{\partial}{\partial z} H^p, \ |\psi| < \delta, \tag{5}$$

where $\xi = 2\pi y/l$, $\delta = \pi d_n/l$ are dimensionless coordinate and half of the strip width, $K(\psi, \xi)$ is a regular kernel function, H^p is so-called primary field and it describes the excitation field.

We discretize (5) using the Nyström-type method [20], [21] with Gauss-Chebyshev quadrature rules, converting the integral equation into a compact system of linear algebraic equations. Solving this system yields the Fourier coefficients of the scattered field and allows one to construct the local reflection r_n and transmission t_n operators.

Coupling via Operator Equations

Once the scattering operators r_n and t_n are determined for all N layers, the electromagnetic response of the entire stack is determined using the operator method for multilayer structures [4]. Unlike standard transfer matrix methods, which may suffer from numerical instability due to exponentially growing terms, we employ a stable recursive system of matrix equations of the second kind.

Let $\mathbf{B}_m$ and $\mathbf{C}_m$ denote the vectors of Fourier amplitudes of the waves propagating upwards (away from the substrate) and downwards (towards the substrate) in the region between the m-th (m+1)-th gratings, respectively (see Fig. 1). The coupling between adjacent layers is governed by the following set of Fredholm second-order matrix equations:

$$\mathbf{B}_m = \mathrm{t}_{m+1}\mathrm{e}_m\mathbf{B}_{m+1} + \mathrm{r}_{m+1}\mathrm{e}_m\mathbf{C}_m, \tag{6}$$

$$\mathbf{C}_m = \mathrm{r}_m\mathrm{e}_m\mathbf{B}_m + \mathrm{t}_m\mathrm{e}_{m-1}\mathbf{C}_{m-1}, \tag{7}$$

where e_m is a diagonal matrix of phase shifts accounting for the propagation of spatial harmonics through the dielectric of thickness $\Delta_m = h_m + h_{m+1}$: $\mathrm{e}_m = \mathrm{diag}\{\exp(i\,\gamma_k \Delta_m)\}$, $k = -\infty...+\infty$.

For a finite stack of N layers, the structure is closed by the radiation conditions at the top and bottom interfaces. The total reflection, **R**, and transmission, **T**, amplitude vectors are expressed as:

$$\mathbf{R} = \mathrm{r}_1\mathrm{q} + \mathrm{t}_1\mathrm{e}_1\mathbf{B}_1, \tag{8}$$

$$\mathbf{T} = \mathrm{t}_N\,\mathrm{e}_N\mathbf{C}_N. \tag{9}$$

For numerical implementation, the operators are truncated by retaining Floquet harmonics with indices $k \in [-M_{tr}, M_{tr}]$, resulting in matrices of size $(2M_{tr} + 1)\times(2M_{tr} + 1)$. Due to the exponential decay of evanescent modes in dielectric

spacers, values $M_{tr}\approx 5–10$ provide sufficient accuracy. The computational cost scales linearly with the number of layers N.

The key advantage of the proposed formulation lies not only in numerical accuracy but also in its ability to serve as an efficient forward solver within large-scale optimization loops. By reducing the electromagnetic problem to a surface-based formulation, the number of unknowns scales with the number of interfaces rather than with the physical volume of the multilayer structure. This makes repeated forward evaluations feasible even for multilayer systems, which is generally impractical for volumetric methods such as the finite-element method (FEM) or the finite-difference time-domain (FDTD) method.

PARALLEL COMPUTATIONAL FRAMEWORK

To efficiently solve the inverse scattering (optimization) problem, which requires evaluating the objective function thousands of times, we developed a heterogeneous parallel computing framework. The system follows a master-slave architecture, leveraging Python's flexibility for the evolutionary algorithm and C++'s raw computational speed for the rigorous electrodynamic solver.

The framework consists of two distinct software components communicating over a TCP/IP network:

The server (Orchestrator) is written in Python. This component manages DE population, handles the genetic operations (mutation, crossover, selection), and dispatches computing jobs to available clients. It uses the asyncio library for non-blocking network communication and threading to separate the DE logic from the graphical user interface (GUI). The clients (solvers) represent the High-performance applications written in C++. Each client acts as a function evaluator. It receives a set of geometric and material parameters, constructs the corresponding scattering matrices, and computes the spectral response.

Both server and client applications have graphical user interfaces (GUI). On the server side, this enables real-time visualization of the convergence curve and dynamic adjustment of DE hyperparameters such as mutation factor, F, crossover rate, CR. On the client side, the GUI provides visual feedback on the current structure-layer profile and field distribution, which is essential for debugging and monitoring the physical validity of the solution.

The core optimization logic resides on the Python server. To maximize resource utilization, the server maintains a pool of connected C++ clients. The DE algorithm is parallelized at the generation level.

During population initialization, the server generates an initial population of NP vectors within the specified bounds. The initialization and subsequent evolution are confined within a hyper-rectangular search space defined by the lower and upper bounds for each parameter, e.g., graphene chemical potential $\mu_{cn} \in [0,\ 1]$ eV, layer spacing $\Delta_n = h_{1,n+1}+h_{2,n}$, where $h_1,\ h_2 \in [\varepsilon_{gap}, h_{\max}]$. A specific geometric constraint is applied to the strip width $2d_n$ to ensure the physical realizability of the periodic structure. To prevent the graphene strips from overlapping with neighboring periods or touching the cell boundaries, the maximum strip width is strictly limited $2d_{\max} = l - \varepsilon_{gap}$, where ε_{gap} is a small safety margin, while the minimum strip width $2d_{\min} = \varepsilon_{gap}$. This constraint is enforced during the trial vector generation and DE execution.

At the job dispatching stage, for each generation G, the server generates trial vectors $\boldsymbol{U}_{i,G}$. These vectors are converted into "jobs" and placed in an asynchronous queue. The job_dispatcher coroutine continuously monitors the status of connected clients and assigns pending jobs to free workers.

A critical feature of our implementation is the strict elitist selection strategy. After all trial vectors in a generation are evaluated, the server compares the trial fitness $F(\mathbf{U}_{i,G})$ with the target fitness $F(\mathbf{X}_{i,G})$, where:

$$\mathbf{X}_{i,G+1} = \begin{cases} U_{i,G}, & \text{if } F(\mathbf{U}_{i,G}) \le F(\mathbf{X}_{i,G}), \\ \mathbf{X}_{i,G}, & \text{otherwise.} \end{cases} \tag{10}$$

Here, $\mathbf{X}_{i,G}$ denotes the parameter vector of the i-th individual in the current population (the target vector). This mechanism ensures that the best traits are preserved ("elitism"), and the global fitness of the population monotonically improves over time. The best individual of each generation is serialized to disk to prevent data loss and allow for result analysis.

The client software is implemented in C++ to ensure maximum execution speed for complex matrix operations. The application listens on a TCP socket for incoming commands. Upon receiving a request, the client performs the following steps. During the parameter loading step, it reads the specific layer configuration (thicknesses and permittivity) from shared storage. During the matrix construction step, it generates truncated scattering matrices of size $(2M_{tr} + 1)\times(2M_{tr} + 1)$. At the recursive solving step, it executes the recursive operator algorithm (7)-(10) to determine reflection and transmission coefficients, as well as absorbance. At the fitness calculation step, it compares the computed spectral characteristics with the required ones using the weighted objective function and returns the result to the server.

To minimize network overhead, we implemented a custom lightweight text-based protocol. Heavy data (such as full layer topology vectors) is exchanged via a shared network file system, while the TCP socket is used exclusively for control commands and synchronization. The communication cycle is defined as follows. Upon connection, the server assigns a unique ClientID to the worker. The server sends a job request in the ASCII format. It sends the specific configuration file location and the dynamic weights for the objective function components. The C++ client uses a

buffered socket reader. It parses the tokenized string, loads the geometry from configuration file, and runs the solver. After computation, the client sends back a concise response.

This approach decouples the data structure complexity from the transmission protocol, allowing us to change the number of layers or parameters without rewriting the network code.

The numerical analysis is performed on a discrete frequency grid $f_k = f_{\min} + k\Delta f$, k=1, 2, ..., M, where M is the number of frequency points, the integral objective function (4) is replaced by a discrete summation of local penalties. The client calculates the total fitness F_1 as:

$$F_1(\mathbf{P}) = \sum_{k=1}^{M} S_1(A(f_k, \mathbf{P})), \tag{11}$$

where $S_1(A)$ is a piecewise linear penalty function defined by a set of thresholds (t_1, ..., t_4) and value parameters (v_1, ..., v_4) received from the server. This function assigns a low penalty value v_1 if the absorbance A exceeds the high threshold t_1, and a maximum penalty v_4 if A falls below the critical threshold t_4. Intermediate values are determined via linear interpolation, allowing for a flexible definition of the optimization goal ("soft" vs "hard" constraints) by simply adjusting the weights in the server configuration,

$$S_1(x) = \begin{cases} v_1, & x \geq t_1, \\ v_2 + \dfrac{x - t_2}{t_1 - t_2}(v_1 - v_2), & t_2 \leq x < t_1, \\ v_3 + \dfrac{x - t_3}{t_2 - t_3}(v_2 - v_3), & t_3 \leq x < t_2, \\ v_4, & x < t_4. \end{cases} \tag{12}$$

NUMERICAL RESULTS AND DISCUSSION

The primary goal of the optimization is to maximize the absorbance $A(f)$ over the frequency band of interest, $f \in [f_{\min}, f_{\max}]$. Namely, our purpose is to maximize absorption, at least at the level $A > 0.8$, preferably $A > 0.95$. For wideband applications, absorption uniformity is as critical as its peak value. Sharp drops in absorbance (where $A \to 0$) due to the excitation of high-Q resonances render the device ineffective. Consequently, the objective function must strictly penalize such spectral holes. The structure under study can support multiple resonances. Resistive graphene strip acts a resonator for the plasmon modes in the terahertz and infrared frequency range. However, at GHz, they are not excited. Periodic structures support Rayleigh anomalies on vacuum or grating modes in a dielectric slab. Also, inter-layer Fabry-Perot modes and corresponding resonances can be excited.

Based on the discrete frequency model (11), we employ a piecewise-linear penalty function with the following empirically determined coefficients: thresholds t_1=1.00, t_2=0.95, t_3=0.80, t_4=0.20, and corresponding values v_1= –5.0, v_2= –0.5, v_3=0.0, v_4=50.0. This configuration creates a "soft" reward for high absorption ($A > 0.95$) and a severe "hard" penalty for any drop below 0.2, effectively guiding the evolutionary search away from solutions with deep reflection resonances.

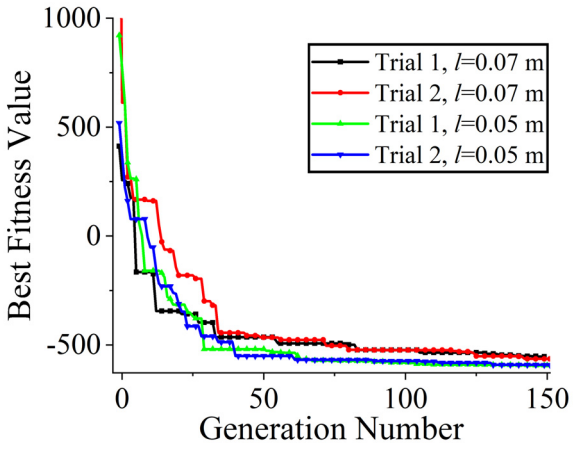

Figure 2. Convergence curves. The best fitness value vs. the generation number for different periods, l = 0.05 m and l = 0.07 m, and two trials, N=10, θ=0^0.

The population consisted of NP=50 individuals. Since DE is a stochastic process, multiple independent runs were performed to avoid stagnation in local optima. Fig. 2 shows convergence curves of the best fitness value versus the generation number. The convergence exhibits a characteristic step-like behavior and typical two distinct phases [10]. In the early stages, we observe large steps corresponding to the "exploration" phase, where the algorithm rapidly discards

clearly non-optimal geometries. In the later stages, the curve shows long plateaus separated by small improvements ("exploitation" phase), as the algorithm fine-tunes the strip widths and chemical potentials to suppress residual resonances.

For the optimization, we take the number of frequency points $M = 250$, the frequency step is $\Delta f = 0.1$ GHz, the frequency band is $f_{min} = 1$ GHz, $f_{max} = 25.9$ GHz, and the number of layers $N = 10$. The relative permittivity of the medium is typical for fighter jet cockpit canopy (polycarbonate), $\varepsilon = 3$. The incidence angle is $\varphi_0 = 90^0$ (orthogonal incidence). The graphene parameters are $\tau = 1$ ps, T = 300 K. The geometric parameters are $h_{max} = 0.7$ m, ε_{gap} is set to 0.01 m in the configuration.

Direct optimization of a 10-layer structure involves a high-dimensional search space (4 parameters × 10 layers = 40 variables), which can lead to slow convergence. To mitigate this, we employ a dimensionality reduction strategy based on cubic spline interpolation. The chromosome (trial vector) of each individual consists of only 16 reference parameters. These correspond to the four physical characteristics (d_n, h_{1n}, h_{2n}, μ_{cn},) defined at four specific "anchor" layers: indices $n = \{1, 4, 7, 10\}$. During the evaluation phase, the server expands this 16-element vector into the full set of 40 parameters for all 10 layers using cubic interpolation (scipy.interpolate.interp1d). This approach ensures a smooth gradient of properties across the stack, which is physically favorable for wideband matching. After the cubic interpolation, the constraints are applied preventing parameters for non- anchor layers to be out of ranges.

All computations are performed on a 12th-generation Intel Core i7 processor (featuring 8 performance and 4 efficiency cores). Electromagnetic simulation for a single individual takes approximately 80 seconds on a single computational thread. The order of the resulting linear algebraic system is 30 for a single layer. Additionally, 21 plane waves (both propagating and evanescent) are considered in the multilayer structure. During the optimization, the efficiency cores were deliberately excluded. The number of parallel threads is strictly limited to 10. Allocation of additional threads increases the computation time per task due to memory access overhead and cache contention among the performance cores. Consequently, evaluation of a single population of 50 individuals in parallel takes approximately 400 seconds. The time required for the differential evolution algorithm operations, task distribution, and data exchange is negligibly small compared to the rigorous electromagnetic simulation.

To visualize the effectiveness of the DE optimization, we compare the spectral response of the best individuals at different stages of the evolutionary process. Fig. 3 presents the power reflection, transmission and absorption coefficients vs. the frequency for the best candidate obtained at the 25th generation (early stage) versus the final solution at the 100th generation. As observed, the solution at the 25th generation already satisfies the basic requirement of $A > 0.8$ over a significant portion of the band. However, the dependencies exhibit highly oscillatory behavior, with several sharp minima where the absorbance drops significantly. These dips typically correspond to the excitation of high-Q resonances within the multilayer structure, which have not yet been fully compensated. Crucially, the final converged solution (100th generation) demonstrates that the algorithm successfully adjusted the geometric and physical parameters to significantly suppress these detrimental resonances. The optimization effectively flattened the spectral response, maximizing the area under the absorbance curve and eliminating the "holes" in the operational band. For a complete optimization run of 100 generations, the total number of objective function calls (forward solver evaluations) is 5000 per trial.

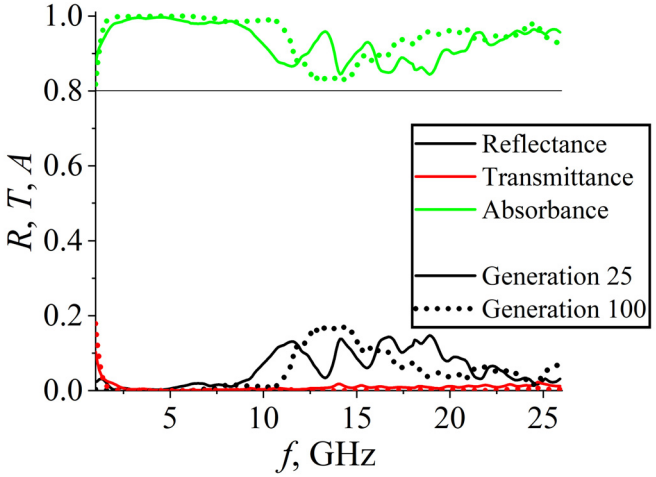

Figure 3. Power reflection, transmission, and absorption coefficients vs. the frequency for the best individuals from the 25th (dashed lines) and 100th (solid lines) generations, $l = 0.05$ m, N=10, θ=0^0

We further investigated the influence of the structure period l on the optimization results. Fig. 4 shows the dependence of the power reflection, transmission, and absorption coefficients on frequency. Two distinct cases are presented in Fig.4, for $l = 0.05$ m and $l = 0.07$ m. The results shown in Fig. 4 indicate that the interpolation-based optimization successfully finds high-absorption solutions in both cases. With a larger period, more resonances can be excited in the considered frequency band, creating a strong perturbation that the optimizer must counteract by precisely

tuning the graphene chemical potential and strip widths. This increased complexity is clearly reflected in the convergence curves shown in Fig. 2. The fitness levels for the structure with the larger period remain consistently higher (indicating a larger penalty) throughout the optimization process. DE algorithm requires more generations to find a specific combination of parameters that can "cancel out" the additional grating-induced resonances. Essentially, each new resonance peak in the spectrum acts as an additional constraint in the parameter space, shifting the global minimum of fitness function $F(\mathbf{P})$ and making the optimization landscape more rugged. Despite this, the final absorbance profiles for both periods reach the target level.

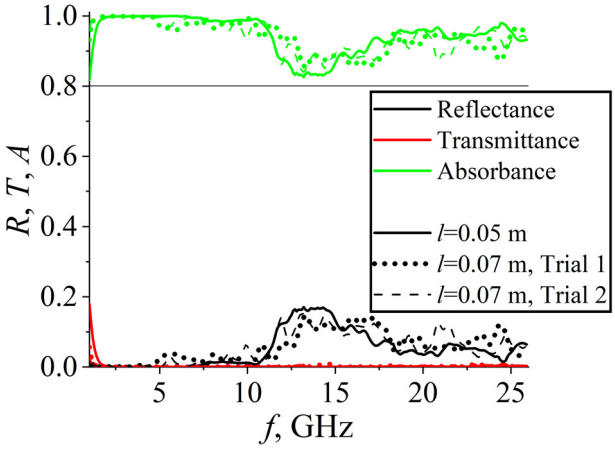

Figure 4. Power reflection, transmission, and absorption coefficients vs. the frequency for different periods l = 0.05 m and l = 0.07 m, N=10, θ=0^0

From a practical engineering perspective, supplying an individual DC bias voltage to each isolated graphene strip in a 10-layer stack presents a significant fabrication challenge. To address this, we performed a constrained optimization run simulating "unbiased" graphene. In this scenario, the chemical potential μ_{cn} was removed from the gene vector and fixed at μ_{cn}=0 eV, leaving only the geometric parameters (strip widths and layer spacings) available for optimization. The results are shown in Fig.5 for 100th generation. As shown, even without active tuning of the chemical potential, the algorithm successfully identifies a geometric configuration that yields substantial absorption.

Finally, we study the angular stability of the optimized 10-layer absorber. Although the structure was optimized for normal incidence ($\theta = 0°$), its performance was evaluated at oblique angles of $\theta = 30°$ and $\theta = 60°$. The results, presented in Fig. 6, demonstrate that the absorbance remains remarkably stable. Except for a narrow frequency range at the lower end of the spectrum, the absorption coefficient remains above the required level of 0.8 even at significant tilt angles. The results indicate that the proposed multilayer configuration possesses high angular tolerance, which is essential for effective electromagnetic shielding and radar-absorbing applications in real-world scenarios.

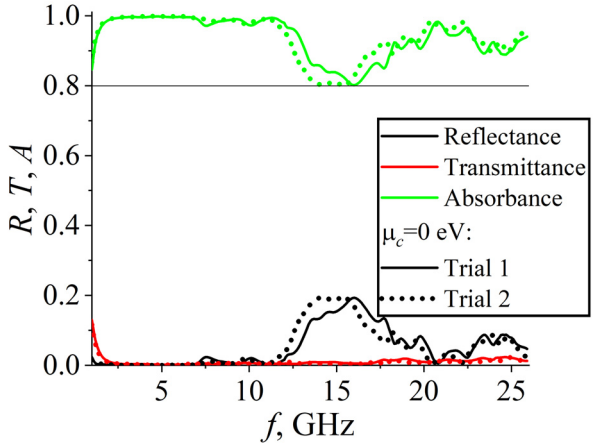

Figure 5. Power reflection, transmission, and absorption coefficients vs. the frequency for unbiased graphene structure, l = 0.05 m, μ_{cn} = 0 eV, N=10, θ=0^0

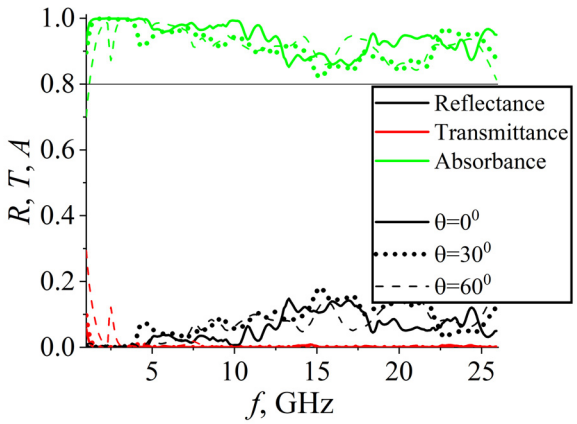

Figure 6. Power reflection, transmission, and absorption coefficients vs. the frequency for different incidence angles θ=0^0, θ=30^0, and θ=60^0, l = 0.07 m, N=10

The angular stability of the optimized structure under oblique incidence is primarily governed by the strips' resistive nature and the applied optimization strategy. The surface conductivity of graphene strips is independent of the angle of incidence. In the microwave range, the localized resonance effects on the isolated graphene strip are less pronounced than in the terahertz frequency range, where high-Q plasmon resonances can arise. Also, the DE optimization process finds a set of parameters that maximally suppresses the resonances connected with the periodicity,

thereby preventing the formation of narrow dips in the frequency dependences. As a result, the absorption mechanism becomes less sensitive to phase variations introduced by oblique incidence, while the contribution of resistive losses remains dominant over a broad angular range.

CONCLUSIONS

The developed surface-based electromagnetic formulation enables efficient analysis of multilayer periodic absorbing structures with a large number of layers, avoiding volumetric discretization of the dielectric domain. By reducing the problem dimensionality to the grating interfaces, the computational cost scales with the number of layers rather than the physical thickness of the structure. As a result, the proposed forward solver is orders of magnitude more efficient than domain-discretization techniques such as FEM or FDTD, making it particularly suitable for repeated evaluations within iterative optimization loops.

Coupling this solver with a parallel differential evolution algorithm allows practical optimization of high-dimensional multilayer designs under broadband performance requirements and fabrication-inspired constraints. The numerical results demonstrate that the optimized ten-layer resistive grating structure provides stable broadband absorption, effectively suppresses resonance-induced spectral holes, and preserves optical transparency and robustness under oblique incidence.

The proposed approach provides a scalable, computationally efficient tool for designing advanced multilayer radar absorbers and can be readily extended to other classes of planar periodic electromagnetic structures and polarization scenarios.

ORCID

Mstyslav E. Kaliberda, https://orcid.org/0000-0002-8169-4360; **Sergey A. Pogarsky,** https://orcid.org/0000-0003-0833-1421

Acknowledgments

The work of S.A.P., V.A.L. was partially supported by the Ministry of Education and Science of Ukraine, grants number 0124U000670, 0126U000999, and that of M.E.K. by the National Research Foundation of Ukraine via project #2025.07/0094.

REFERENCES

[1] E.F. Knott, J.F. Shaeffer, and M.T. Tuley, *Radar Cross Section*, 2nd ed. (Scitech Publishing Inc., Raleigh, NC, USA, 2004).
[2] B.A. Munk, *Frequency Selective Surfaces: Theory and Design*, (John Wiley & Sons, Inc., New York, 2000), 410 p.
[3] M.E. Kaliberda, L.M. Lytvynenko, and S.A. Pogarsky, J. Opt. Soc. Amer. A. **36**(10), 1787 (2019). https://doi.org/10.1364/JOSAA.36.001787
[4] M.E. Kaliberda, L.M. Lytvynenko, and S.A. Pogarsky, Int. J. Microw. Wireless Technol. **12**(5), 380 (2020). https://doi.org/10.1017/S1759078719001430
[5] R.P.S. Bhadoriya, V. Bajaj, and R. Panwar, in: *2023 International Conference on Electrical, Electronics, Communication and Computers (ELEXCOM)*, edited by R. Roorkee, (IEEE, Roorkee, India, 2023), pp. 1-4.
[6] R. Storn, and K. Price, J. Glob. Optim. **11**(4), 341 (1997). https://doi.org/10.1023/A:1008202821328
[7] S. Wang, A. Zhou, and Y. Zhang, Chin. J. Electron. **34**(3), 871 (2025). https://doi.org/10.23919/cje.2023.00.322
[8] I. Farda, A. Thammano, and J. Morris, IEEE Access. **12**, 131809 (2024). https://doi.org/10.1109/ACCESS.2024.3460385
[9] Z. Cai, S. Gao, X. Yang, and M. Zhou, IEEE Trans. Syst. Man Cybern. Syst. **54**(12), 7318 (2024). https://doi.org/10.1109/TSMC.2024.3447051
[10] J. de Jesús Rubio, IEEE Trans. Neural Netw. Learn. Syst. **36**(8), 14201 (2025). https://doi.org/10.1109/TNNLS.2025.3526580
[11] D. Cai, *et al*., IEEE Sens. J. 23(20), 25271 (2023), https://doi.org/10.1109/JSEN.2023.3311467
[12] P. Singh, and R.S. Hegde, IEEE Antennas Wirel. Propag. Lett. **24**(11), 3986 (2025). https://doi.org/10.1109/LAWP.2025.3598331
[13] K. Dutta, M.O. Akinsolu, P. Kumar Mishra, B. Liu, and D. Guha, IEEE Open J. Antennas Propag. **5**(3), 693 (2024). https://doi.org/10.1109/OJAP.2024.3385675
[14] F. Lan, *et al*., IEEE Trans. Plasma Sci. 52(7), 2991 (2024). https://doi.org/10.1109/TPS.2024.3412995
[15] M. Zhai, *et al*., IEEE Antennas Wirel. Propag. Lett. **23**(10), 3043 (2024). https://doi.org/10.1109/LAWP.2024.3421549
[16] F. Peng, X. Chen, and J. Xue, IEEE Trans. Antennas Propag. **73**(7), 4384 (2025). https://doi.org/10.1109/TAP.2025.3553761
[17] L. Zuo, Z. Liang, and Y. Long, IEEE Antennas Wirel. Propag. Lett. **24**(6), 1367 (2025). https://doi.org/10.1109/LAWP.2025.3537215
[18] G.W. Hanson, J. Appl. Phys. **103**, 064302 (2008). https://doi.org/10.1063/1.2891452
[19] G.W. Hanson, IEEE Trans. Antennas Propag. **56**, 747 (2008). https://doi.org/10.1109/TAP.2008.917005
[20] Yu.V. Gandel, and V.D. Dushkin, J. Math. Sci. **212**, 156 (2015). https://doi.org/10.1007/s10958-015-2656-2
[21] M.E. Kaliberda, S.A. Pogarsky, and A.A. Sierhieieva, Opt. Quantum Electron. **55**, 1050 (2023). https://doi.org/10.1007/s11082-023-05288-5

ОПТИМІЗАЦІЯ БАГАТОШАРОВОГО ПОГЛИНАЧА НА БАЗІ ГРАФЕНУ У ВИПАДКУ Н-ПОЛЯРИЗАЦІЇ З ВИКОРИСТАННЯМ ДИФЕРЕНЦІАЛЬНОЇ ЕВОЛЮЦІЇ В ГІБРИДНОМУ ОБЧИСЛЮВАЛЬНОМУ СЕРЕДОВИЩІ

Мстислав Є. Каліберда[1,2], Сергій О. Погарський[1,2], Владислав М. Насонов[1], Вікторія А. Луньова[1]
[1]Харківський національний університет імені В. Н. Каразіна, майдан Свободи, 4, Харків, Україна, 61022
[2]Радіоастрономічний інститут НАН України, вул. Мистецтв, 4, Харків, Україна, 61002

Представлено обчислювально ефективну методику оптимізації багатошарових радіопоглинаючих структур на основі періодичних плоских решіток з резистивних стрічок, розташованих у діелектричному шарі, для випадку *H*-поляризації. Електромагнітні характеристики моделюються з використанням строгого методу сингулярних інтегральних рівнянь у поєднанні з операторним методом, що забезпечує високу точність і числову стабільність за низьких обчислювальних витрат. Цей надшвидкий алгоритм розв'язання прямої задачі інтегровано в паралельну систему оптимізації на основі диференціальної еволюції, реалізовану в архітектурі клієнт–сервер, що дозволяє ефективно розв'язувати багатовимірні задачі зворотного проєктування. Оптимізація спрямована на досягнення широкосмугового поглинання за нормального падіння зі збереженням оптичної прозорості. Як репрезентативний резистивний матеріал використано графен. Числові результати демонструють ефективне придушення резонансних провалів у спектрі та стабільне широкосмугове поглинання для десятишарових структур, а також стійкість характеристик за умов похилого падіння та з урахуванням конструктивних обмежень.

Ключові слова: *графен; широкосмуговий поглинач; диференціальна еволюція; сингулярне інтегральне рівняння; багатошарова періодична структура; глобальна оптимізація*